Ⓔ

Self-Noise Models of Seismic Instruments

A. T. Ringler and C. R. Hutt

U. S. Geological Survey, Albuquerque Seismological Laboratory

Online material: Sensor test data

INTRODUCTION

Based on coherence analysis methods we develop a method for computing low self-noise models of seismic sensors. We calculate self-noise models for 11 different production seismometers. This collection contains the majority of sensors currently in use at Global Seismographic Network Stations. By developing these noise models, with a standard estimation method, we are able to make absolute comparisons between different models of seismic sensors. This also provides a method of identifying quality variations between two or more of the same model sensor.

Studying Earth's free oscillations requires a large amount of seismic data with a high signal-to-noise ratio at long periods (Laske 2004). Recent tomographic studies using ambient seismic noise (Shapiro *et al.* 2005) also require the self-noise of seismic instruments to be below that of the Earth's ambient background noise, because as they use Earth noise as the seismic signal. It is also important when making temporary sensor deployments that the instrument's noise levels are below that of the signals being used in the study (Wilson *et al.* 2002). In order to verify that seismic instruments meet the above demands and other user requirements it is important from a testing standpoint, that one be able to measure the self-noise of seismic sensors and develop baselines for different models of seismic instruments.

The different methods used to estimate self-noise of seismic sensors have made it difficult to do side-by-side comparisons of their performance (Hutt *et al.* 2009). This lack of a self-noise estimate standard makes it difficult to assess when a sensor's self-noise is above the manufacturers' specifications, indicating a possible problem with the sensor or noisy site conditions. In sensor development it is important to be able to compare a prototype sensor's self-noise to that of known self-noise levels of a reference sensor. On top of these complications some sensor self-noise models are based on theoretical models, which can over- or under-account for noise contributions to the sensor self-noise (Rodgers 1994).

With the above in mind, we propose a method to standardize self-noise estimates for seismic sensors and we calculate the self-noise of 11 different seismic sensors. Our hope is that this will lead to robust estimates of sensor self-noise for use in sensor development, verifying sensor quality, and give overall characterizations of current sensor performance by model. We hope that the instrument self-noise models will be a useful tool to people working in seismic instrumentation and will contribute to the effort of continually increasing seismic data quality.

METHODS

We developed noise models for 11 different seismic sensors, including all models of sensors currently in use at Global Seismic Network (GSN) stations except for Geotech's KS-36000, which is currently in limited use. These models were constructed from noise measurements of 25 different noise tests (Table 1). All of these tests were conducted at the Albuquerque Seismological Laboratory (ASL), which is known to have low ambient background noise (McNamara *et al.* 2004).

We tested both vault and borehole type sensors. All vault sensor tests were conducted in the ASL underground test vault in order to minimize ambient background noise. To increase high-frequency coherency we collocated sensors on a granite slab whenever possible. Our borehole tests were done in the ASL test borehole, which is located near GSN station ANMO (~30 m separation). In all of the tests we used the three-channel coherence analysis estimate (Sleeman *et al.* 2006) to measure the self-noise of the instruments (Figure 1). The three-channel coherence analysis estimate gives good self-noise estimates in a large frequency band (Ringler *et al.* forthcoming). However, if one is only interested in self-noise at long periods, one may also use the two-sensor coherence analysis (Holcomb 1989).

The details of our processing method are as follows: for each broad-band sensor test we visually inspected for approximately 10 hours of non-stop quiet data on the BH and LH vertical channels, which are sampled at 20 or 40 samples per second (sps) and 1 sps, respectively. We then interpolated the data, in the frequency domain, to 40 sps and 8 sps, respectively (Welch 1967). We computed power spectra and cross-power spectra between all sensors, in a given test, by way of the modified Welch method. Our Welch method uses a Hanning window taper for windows that contain 64,000 points with 87% overlap (Figure 1). We used a very large amount of overlap to remove the need for excessive smoothing. Once the BH and LH channel noise levels have been computed, we use the BH data channel noise values for frequencies higher than 0.0075 Hz and we use the LH data channel for frequencies lower than 0.0075 Hz. By using two different sample rates, we were able to extend the frequency band for which the self-noise estimates remain valid without having to increase the time series of the test (Figure 1). We have not smoothed for any discontinuities;

TABLE 1

Different noise test configurations used for constructing noise models. All tests were run for multiple days to ensure the sensors had settled. The right column indicated if any special configurations were used. All tests included recording vertical component output. Test 9 included data from a reference sensor whose self-noise measurement was not included at the request of the vendor.

| Test	Sensor 1	Sensor 2	Sensor 3	Notes
1	STS-2 HG	STS-2 HG	STS-2 HG	2 with wool caps, 1 in bell jar
2	STS-2 HG	STS-2 HG	STS-2 HG	3 with wool caps
3	STS-2 HG	STS-2 HG	STS-1	STS-2s with wool caps
4	STS-2 HG	STS-2 HG	T-240	STS-2s with wool caps, T-240 in stock pot
5	STS-2 HG	STS-2 HG	T-240	STS-2s with wool caps, T-240 in plastic shield
6	STS-2 HG	STS-2 HG	T-240	STS-2s with wool caps, T-240 in plastic shield and styrofoam box
7	STS-2 HG	STS-2 HG	STS-2 HG	1 with wool cap, 1 in sand
8	KS-1	STS-2 HG	STS-1	STS-2 in fiberglass jacket, STS-1 has Metrozet feedback box
9	—	—	STS-1	STS-1 has Metrozet feedback box
10	KS-2000	STS-2 HG	T-240	
11	STS-1	STS-1	STS-2 HG	
12	T-240	T-240	T-240	
13	T-240	T-240	STS-2 HG	
14	T-CMPT	STS-2 HG	STS-2 HG	
15	T-120P	T-120P	T-120P	
16	STS-1	STS-1	CMG-3T	
17	STS-1	STS-1	STS-2 HG	
18	T-120P	T-240	T-240	
19	KS-54000	KS-54000	CMG-3TB	Borehole test
20	CMG-3TB	CMG-3TB	KS-54000	Borehole test
21	GS-13	GS-13	GS-13	
22	KS-54000	CMG-3TB	CMG-3TB	Borehole test
23	151-120	151-120	151-120	
24	151-120	151-120	151-120	
25	151-120	151-120	151-120	

instead we judiciously picked a frequency to overlap, at which there were minimal changes in the power levels between the BH and LH data. The processing techniques used for our instrument self-noise models are discussed in detail in Ringler *et al.* (forthcoming) and Evans *et al.* (2010).

Having computed self-noise estimates for each test, we then take the minimum self-noise for all of the self-noise tests together as a function of frequency for a given model of sensor (*e.g.*, we use the three obtained in Figure 1 along with 23 other self-noise estimates for the STS-2 self-noise model). In each case, we have included the number of self-noise estimates used in the instrument's model figure. This is the low-noise model for the sensor. We also calculate a median self-noise model for each sensor, which is computed by taking the median self-noise from all of the tests of a given model of sensor as a function of frequency. Finally, we apply a 25% logarithmic smoothing (see the Appendix) to both the low-noise and the median self-noise to construct the final instrument self-noise models. By applying a large amount of smoothing, our models had minimal local variations in the self-noise. To increase the robustness of our self-noise models, we used multiple self-noise estimates from a given test

along with multiple tests. Finally, we compared our self-noise models to theoretical self-noise models, when available, and also the Peterson new low noise model (Peterson 1993) for reference.

We have also constructed a self-noise model for the primary model of short-period sensor in use at GSN stations, Geotech's GS-13. In this case, we used only EH channel data which is sampled at 200 sps. For this model we still used the same taper, window size, and overlap. Since our estimate only used 200 sps data, the self-noise estimates are only good at frequencies higher than approximately 0.01 Hz.

Although the above method appears to give good estimates for the self-noise of a particular model of instrument, there are some limitations to the method (Wielandt 2002). First, all coherence analysis methods for calculating self-noise assume that all the sensors in the analysis have a common input signal from the Earth. This requires that the sensors under test be adjacent to each other (within about 0.1 wavelength). For measuring self-noise of borehole sensors, this assumption can be violated at short periods because of local geology and also the distance between the boreholes. Second, small misalignments between seismometers can result in large self-noise estimates (Holcomb
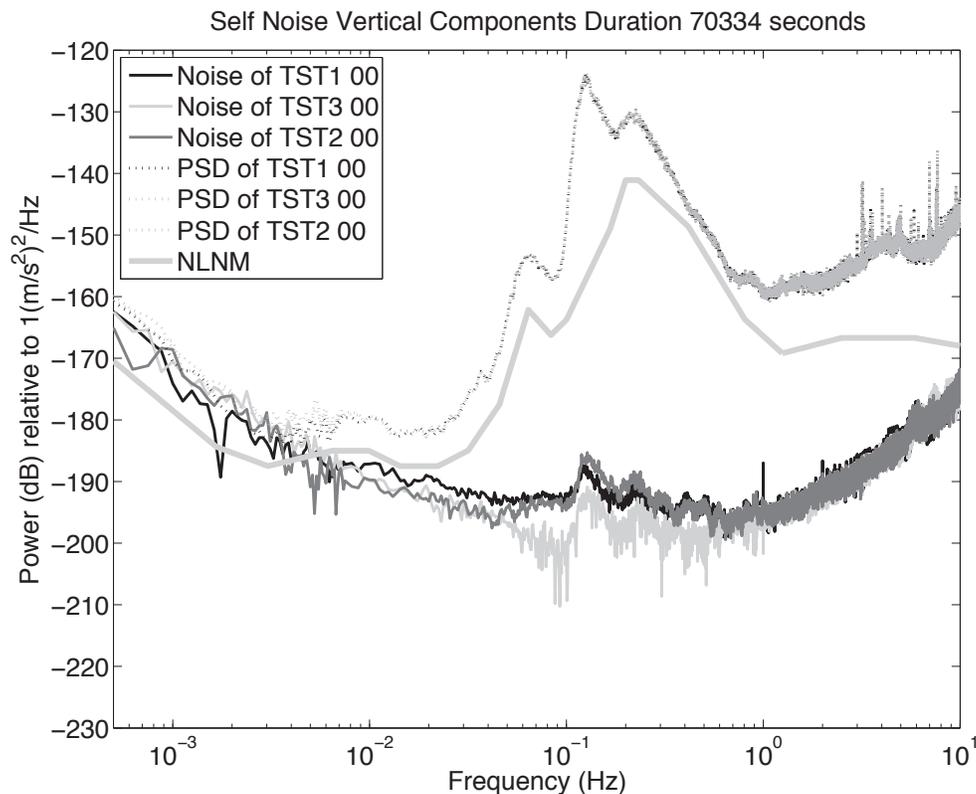
▲ Figure 1. Power spectra and self-noise for three collocated Streckeisen STS-2 vertical seismometers from one test (Test 1, Table1), which were used for making the self-noise models of the STS-2 (TST1 was in a bell jar, TST2 and TST3 were covered with wool caps). We have not done any post-process smoothing to these self-noise estimates. A possible explanation for the elevated noise levels between 1 Hz and .1 Hz could come from inaccuracies in the sensors' level bubbles.

1990). This becomes apparent in the 0.1 Hz to 1 Hz frequency band (Figure 1), where even vertical components see elevated noise in the microseism band. A possible cause of this is limitations in the manufacturing methods. Small misalignments greatly contribute to horizontal self-noise estimates. Third, variable quality between sensors of a given model and variations in the installation methods can produce differences in the self-noise estimates (Ringler *et al.* forthcoming).

RESULTS

We now discuss the 11 self-noise models constructed in our study. When available, we compare our self-noise models with theoretical self-noise models, as specified by the manufacturer. We have also calculated the self-noise for the two models of digitizers used in the study: Quanterra Q680 and Quanterra Q330HR (Quanterra 1993, 2007). For all tests using the Q330HR, the pre-amplifier gain was set to either X1 gain or X20 gain. Our choice for setting the pre-amplifier gain was based on the instrument's sensitivity. However, the end results were likely not changed by the pre-amplifier gain settings, in either case, since the digitizer noise was always well below the instrument self-noise. We calculated the self-noise of the digitizers using a shorted input or a terminated input of 120 ohms from each side to ground. In all cases, the digitizer self-noise was below that of the seismometer for the respective test.

For clarity we have included only the self-noise of the digitizer used in the largest number of tests for a given seismometer model. To allow for a comparison of the noise, we have corrected the self-noise of the digitizer by the instrument response of the given seismometer.

Guralp CMG-3T/CMG-3TB

The Guralp CMG-3TB is the secondary borehole sensor used at GSN stations. It has a flat velocity response from 120 seconds to 50 Hz (Guralp Systems 2006). The self-noise model for this instrument (Figure 2) was constructed from 15 power spectra during three different tests (Table 1). These tests included a total of four different CMG-3T/CMG-3TB sensors. We did not differentiate between the two models of instrument as they appear to have similar self-noise characteristics. There was no theoretical noise model for this sensor.

Geotech GS-13

The Geotech GS-13 is the primary short-period instrument used at GSN stations. It has a natural frequency of 0.75 Hz to 1.1 Hz, which is usually set at 1 Hz (Geotech 1999). We compared our calculated self-noise model (Figure 3) to the theoretical noise model of a GS-13 operating with a Linear Technology LT1012 operational amplifier (Rodgers 1994). In total we used 12 power spectra from one test (Table 1) from three different GS-13 sensors.
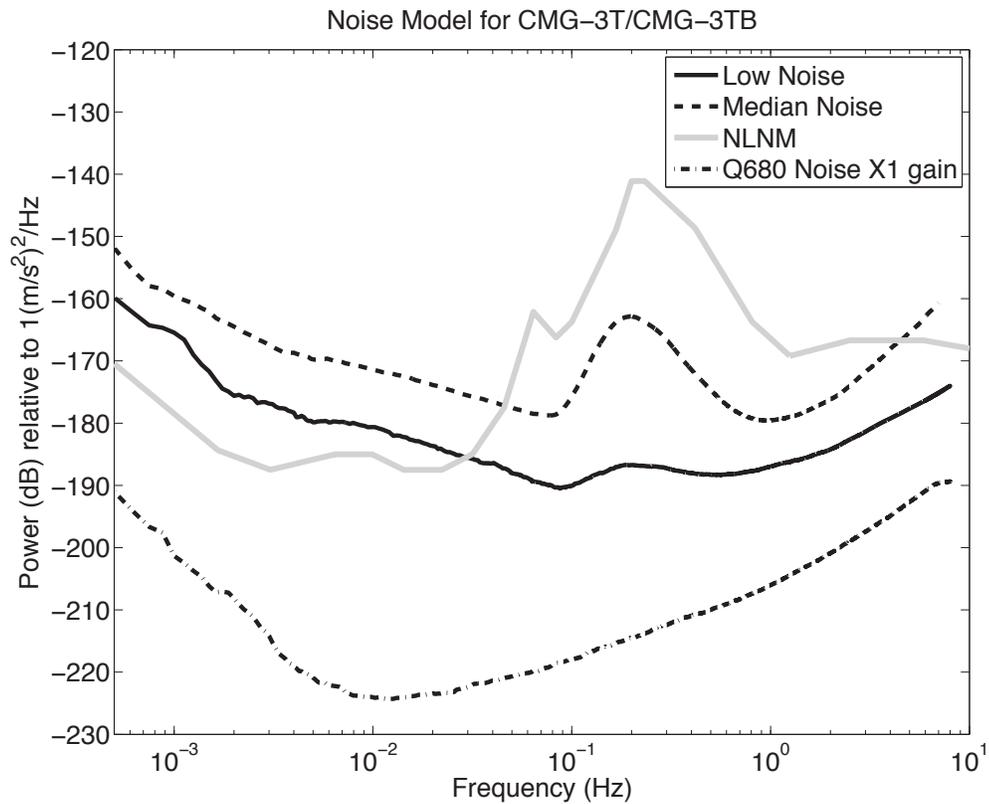
▲ **Figure 2.** Self-noise model of the Guralp CMG-3T/CMG-3TB broadband sensor.
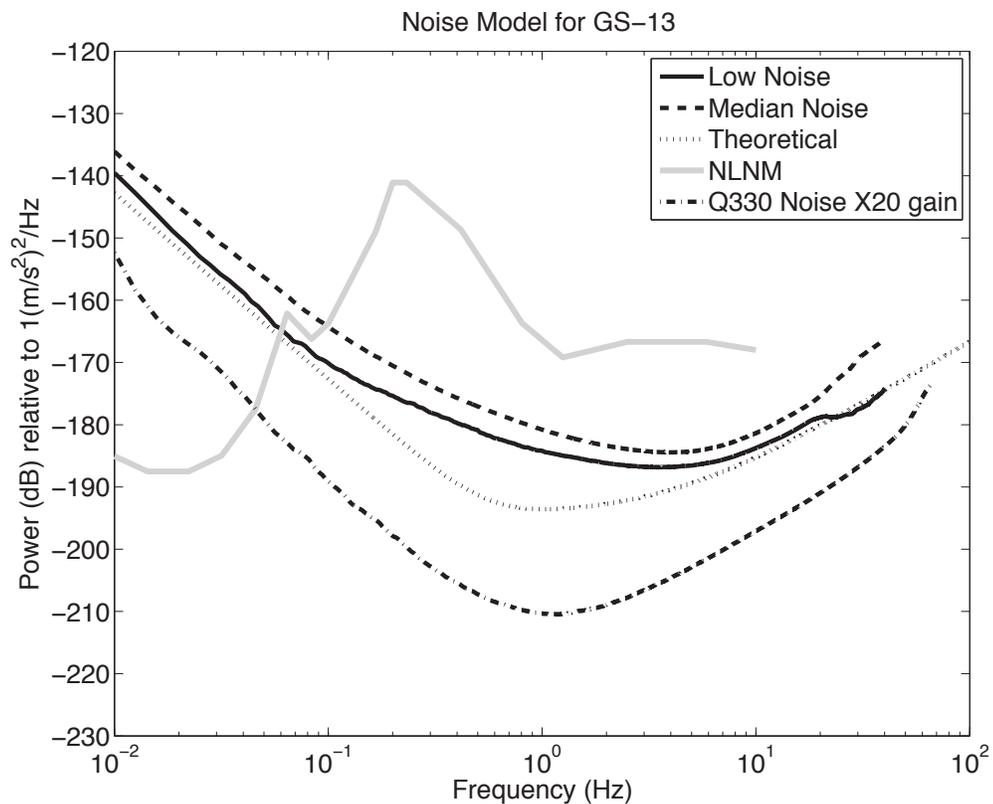
▲ **Figure 3.** Self-noise model for the Geotech GS-13 short-period instrument. The theoretical self-noise is for the GS-13 seismometer connected to a Linear Technology LT1012 operational amplifier.

Geotech KS-1

The Geotech KS-1 is a vault version of the KS-54000 sensor. This sensor has a flat velocity response from 0.003 Hz to 5 Hz (Geotech 2004). As we were only able to acquire one vertical time series test, we have also included horizontal records in the construction of the self-noise (Figure 4). The inclusion of horizontal data could contribute to an elevated instrument noise-model. However, the KS-1's self-noise model is similar to the KS-54000's self-noise model (Figure 5), as we would expect. We have not constructed a median self-noise model because of the limited amount of data. Our model was constructed using three power spectra from one sensor. We compared our calculated self-noise model to the theoretical noise model of the KS-54000.

Geotech KS-2000

The Geotech KS-2000 is a compact version of the KS-54000. The KS-2000 has a flat velocity response from 120 seconds to 50 Hz (Geotech 2006). In our tests only the vault version was tested. As we were only able to acquire two vertical time series tests, we have included horizontal records. Therefore, the median self-noise model is probably elevated slightly. The self-noise model for this instrument (Figure 6) was constructed from eight power spectra during one test (Table 1) of a single KS-2000. There was no theoretical noise model for this sensor.

Geotech KS-54000

The Geotech KS-54000 is the primary borehole sensor used at GSN stations. The KS-54000 is a borehole version of the KS-1

sensor. The sensor has a flat velocity response from 0.003 Hz to 5 Hz (Geotech 2004). We compared our calculated self-noise model (Figure 5) to the theoretical noise model of the KS-54000. Our self-noise model for the KS-54000 used a total of 11 power spectra from two different sensors during three different tests.

Nanometrics Trillium 120P

The Nanometrics Trillium 120P broadband seismometer is a vault style seismometer. The sensor has a flat velocity response from 120 seconds to 175 Hz (Nanometrics 2006). To calculate the self-noise (Figure 7) of the Trillium 120P we used five power spectra during two tests (Table 1) from five different Trillium 120P sensors.

Nanometrics Trillium 240

The Nanometrics Trillium 240 broadband seismometer is a vault style seismometer. This sensor has a flat velocity response from 244 seconds to 207 Hz (Nanometrics 2005). Our self-noise model (Figure 8) for the Trillium 240 was calculated from 11 power spectra during seven tests (Table 1) from four different sensors.
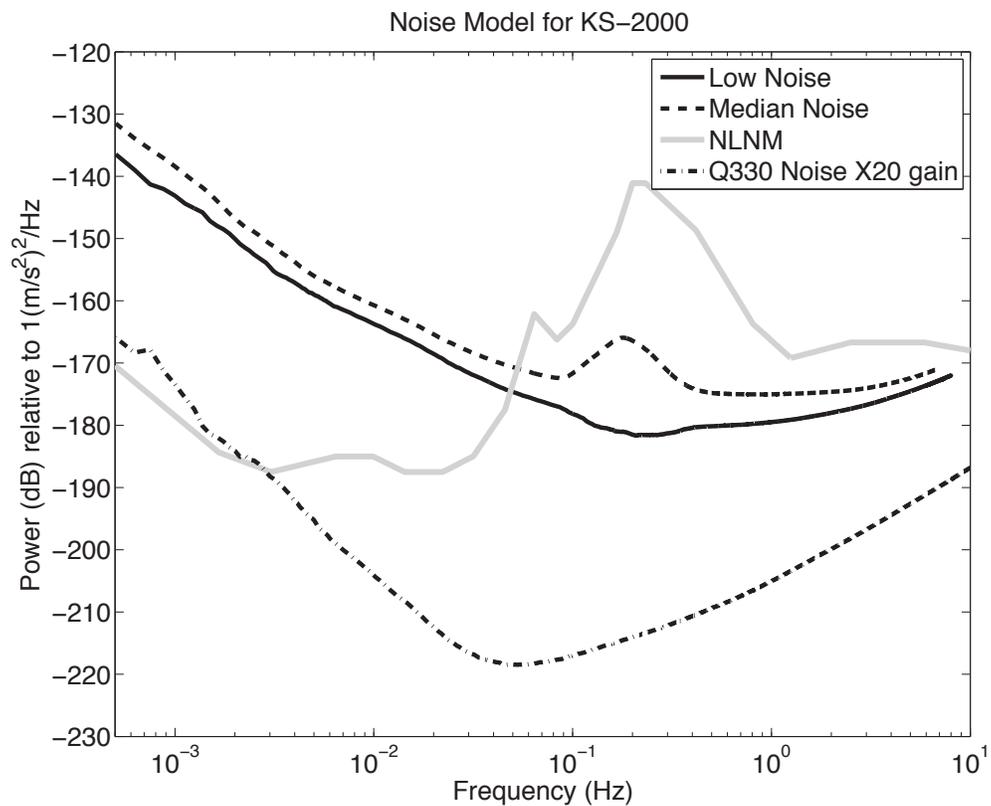
Nanometrics Trillium Compact

The Nanometrics Trillium Compact broadband seismometer is a vault style seismometer. The sensor has a flat velocity response from 120.2 seconds to 108 Hz (Nanometrics 2009). Our self-noise model (Figure 9) for the Trillium compact was
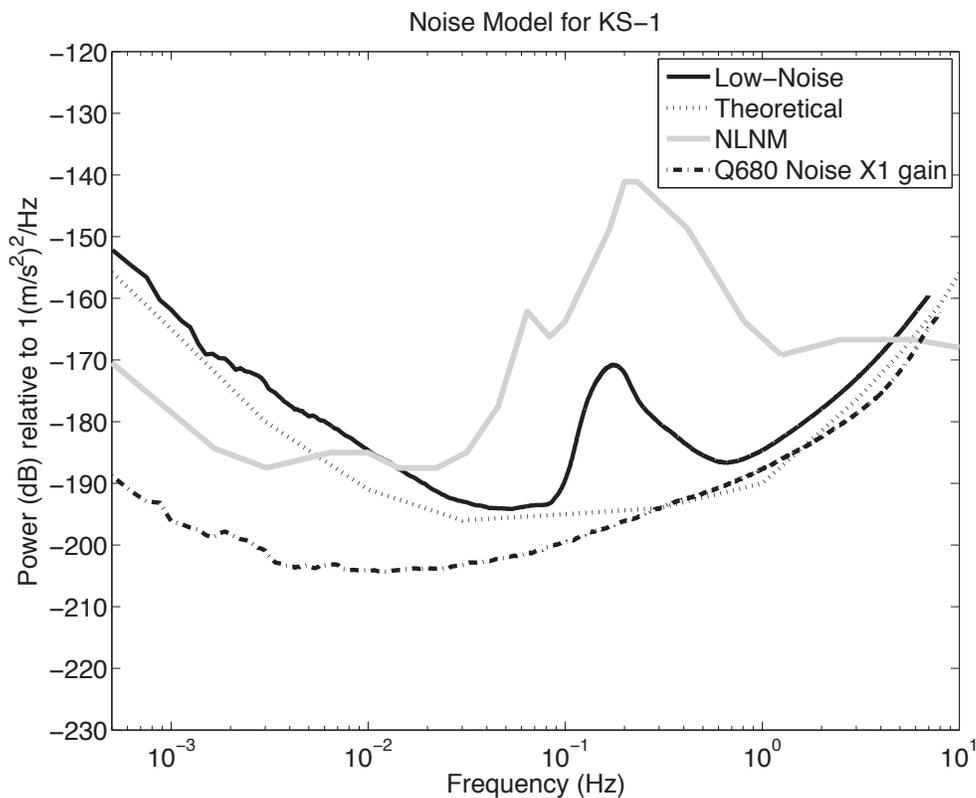

▲ **Figure 4.** Self-noise model of the Geotech KS-1 vault seismometer. This model includes horizontal data because we were unable to get multiple quiet vertical component time series because of the limited number of tests conducted with this model of sensor.
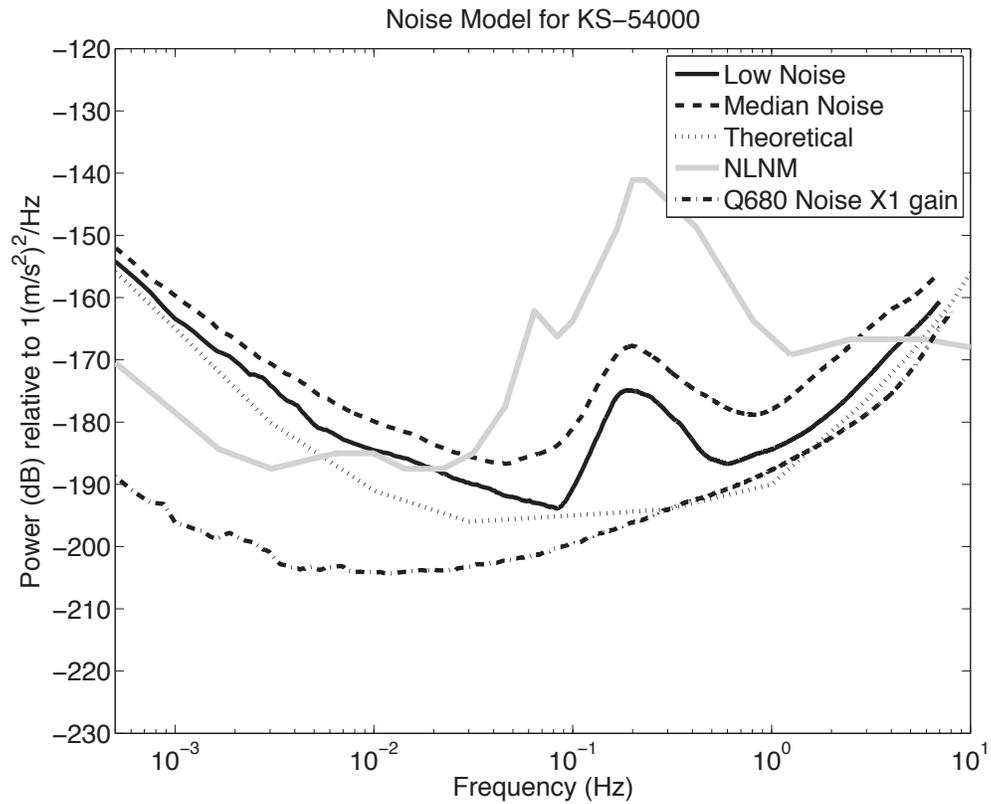
▲ **Figure 5.** Self-noise models for the KS-54000 compared to the theoretical self-noise for the KS-54000.


▲ **Figure 6.** Self-noise model for the Geotech KS-2000 broadband seismometer. This self-noise model includes horizontal component data because of insufficient vertical data.
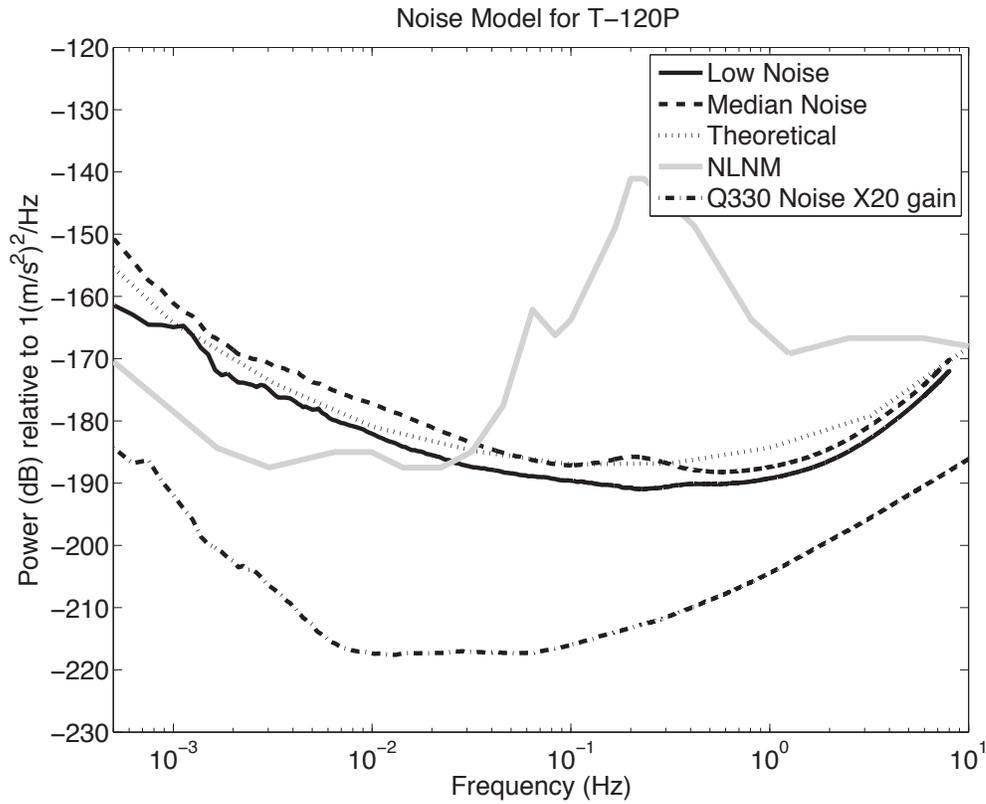
▲ **Figure 7.** Self-noise model for the Nanometrics Trillium 120P broadband seismometer compared to the theoretical noise model.
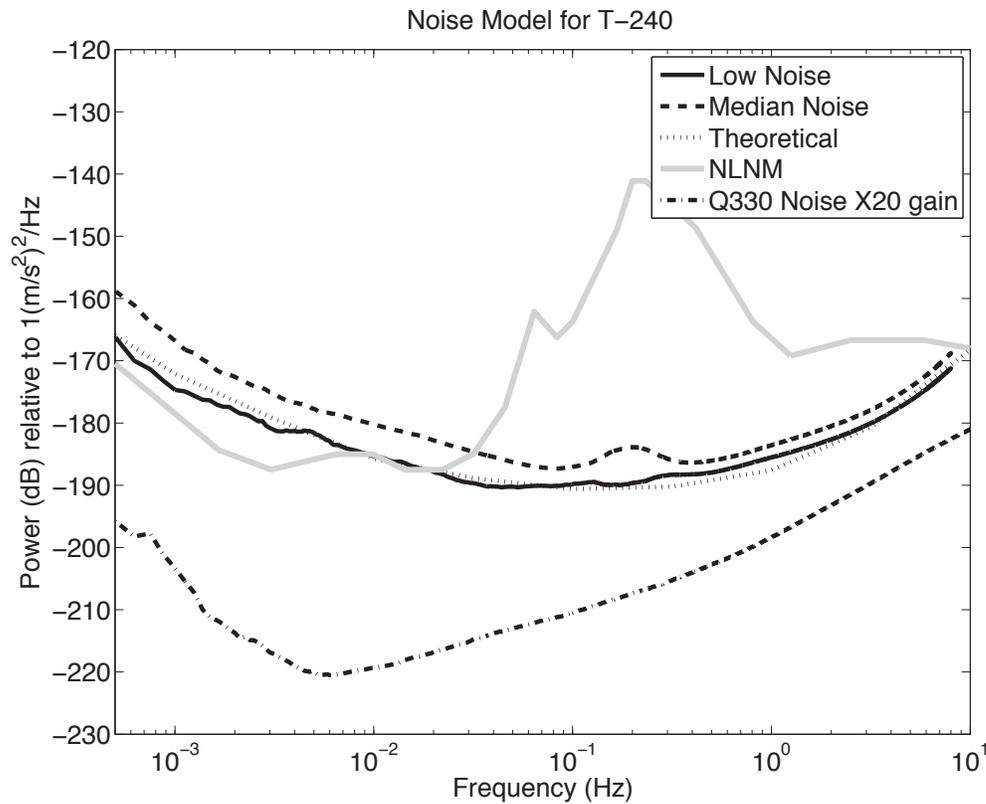
▲ **Figure 8.** Self-noise model of the Nanometrics Trillium 240 broadband seismometer. We have compared our self-noise model with theoretical self-noise supplied by Nanometrics for this seismometer.
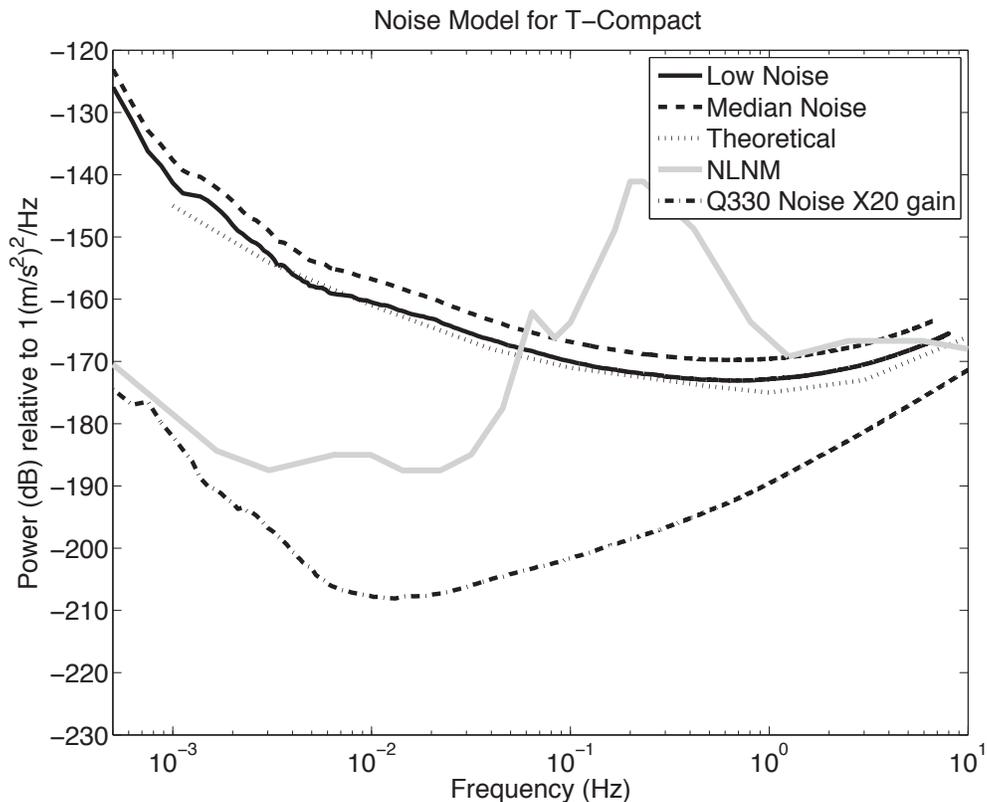
▲ **Figure 9.** Self-noise model of the Nanometrics Trillium compact seismometer compared to its theoretical noise model.

calculated from six power spectra during one test (Table 1) using one sensor.

Ref Tek 151-120

The Ref Tek 151-120 broadband seismometer is a vault style seismometer. The sensor has a flat velocity response from 120 seconds to 50 Hz (Ref Tek 2010). Our self-noise model (Figure 10) for the Ref Tek 151-120 was calculated from nine power spectra during three tests (Table 1) from five different sensors.

Streckeisen STS-1

The Streckeisen STS-1 broadband seismometer is the primary vault style sensor used at GSN stations. The STS-1 seismometer has a flat velocity response from 360 seconds to 10 Hz (Streckeisen 1987). Our self-noise model (Figure 11) for the STS-1 was calculated from 16 power spectra during six tests (Table 1) from four different sensors. A possible explanation for our instrument self-noise model being below the theoretical model at high frequencies could be from lower electronics noise in the new Metrozet E300 replacement feedback boxes, which were used in several of the STS-1 tests.

Streckeisen STS-2 HG

The Streckeisen STS-2 high gain (HG) broadband seismometer is the main secondary vault style sensor used at GSN stations. The STS-2 HG seismometer has a flat velocity response from 120 seconds to >50 Hz (Streckeisen 1995). Our self-noise model (Figure 12) for the STS-2 HG was calculated from 25 power spectra during 13 tests (Table 1) using eight different

sensors. A possible explanation for our instrument self-noise model being below the theoretical model at high frequencies could be from improved sensor electronics in newer STS-2 HGs.

DISCUSSION

We constructed self-noise models from 11 different models of seismometers, including 10 broadband and one short period instrument (Figure 13 and Figure 14). Our 11 different self-noise models included all models of sensors that are currently in operation at GSN stations, except for the KS-36000. Although the number of tests and power spectra for various sensors differed, in all cases we attempted to use enough different power spectra to give a good estimate of the self-noise of the particular model of sensor. Although a "good estimate" is a subjective measure, we found that the computed self-noise models did not change dramatically when we increased the number of power spectra used. That is, a self-noise model for a particular sensor computed with only a few power spectra (*e.g.*, fewer than five) did not differ much from using a lot of power spectra (*e.g.*, more than 20).

One of the important factors in calculating self-noise models is to use power spectra from time periods with low noise. This is why all power spectra used, for broadband seismometer noise model estimates were low-pass filtered and visually inspected to have no large signals (*e.g.*, earthquakes).

The requirement that the power spectra be computed during quiet time segments comes from the limitations of the
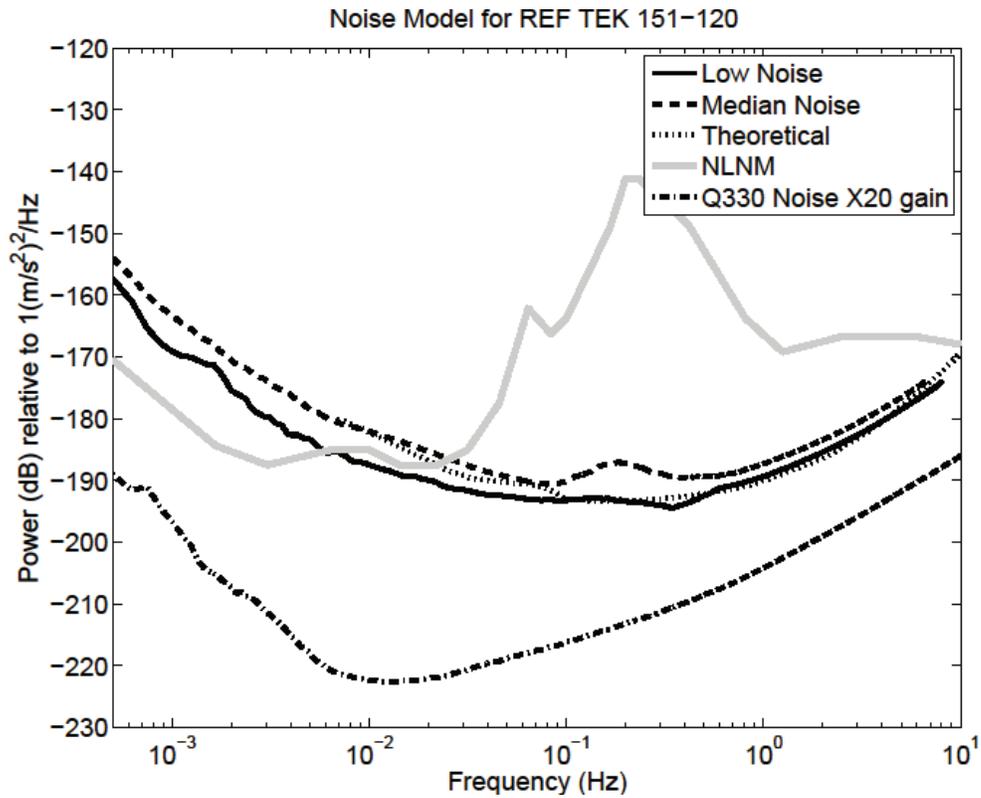
▲ **Figure 10.** Self-noise model of the Ref Tek 151-120 broadband seismometer compared to its theoretical noise model.
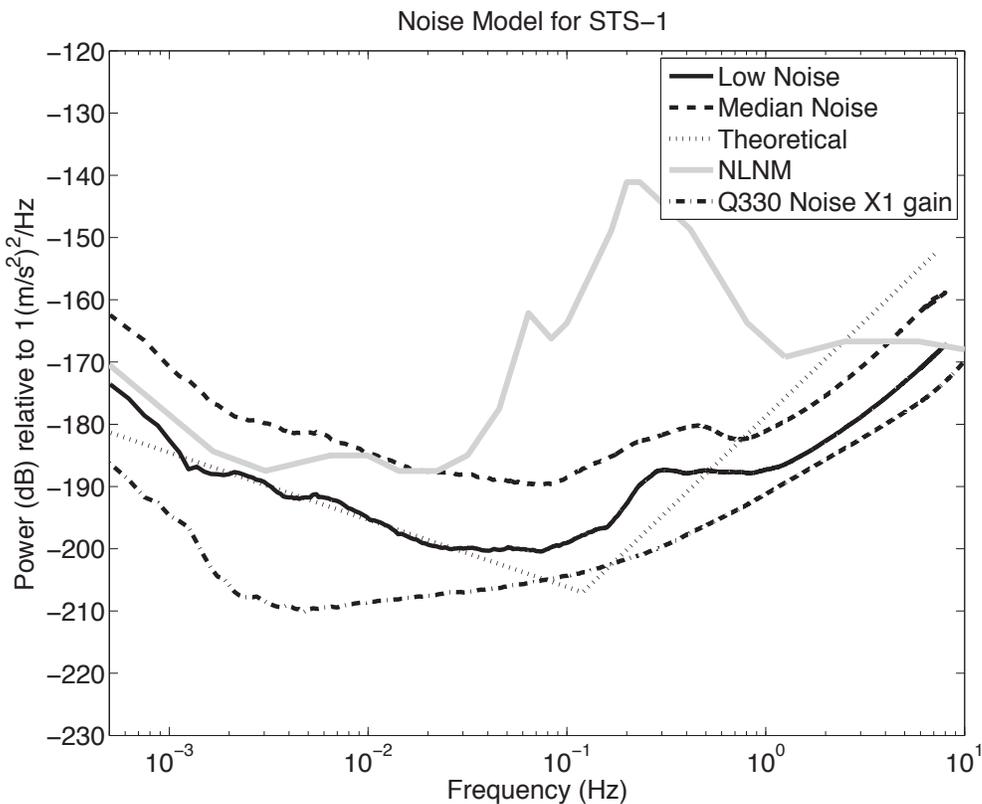
▲ **Figure 11.** Self-noise model of the Streckeisen STS-1 seismometer as compared to the theoretical self-noise of the STS-1. The self-noise model being lower than the theoretical model at high frequencies could possibly come from using the new Metrozet E300 feedback boxes, which appear to have lower high-frequency electronic noise.
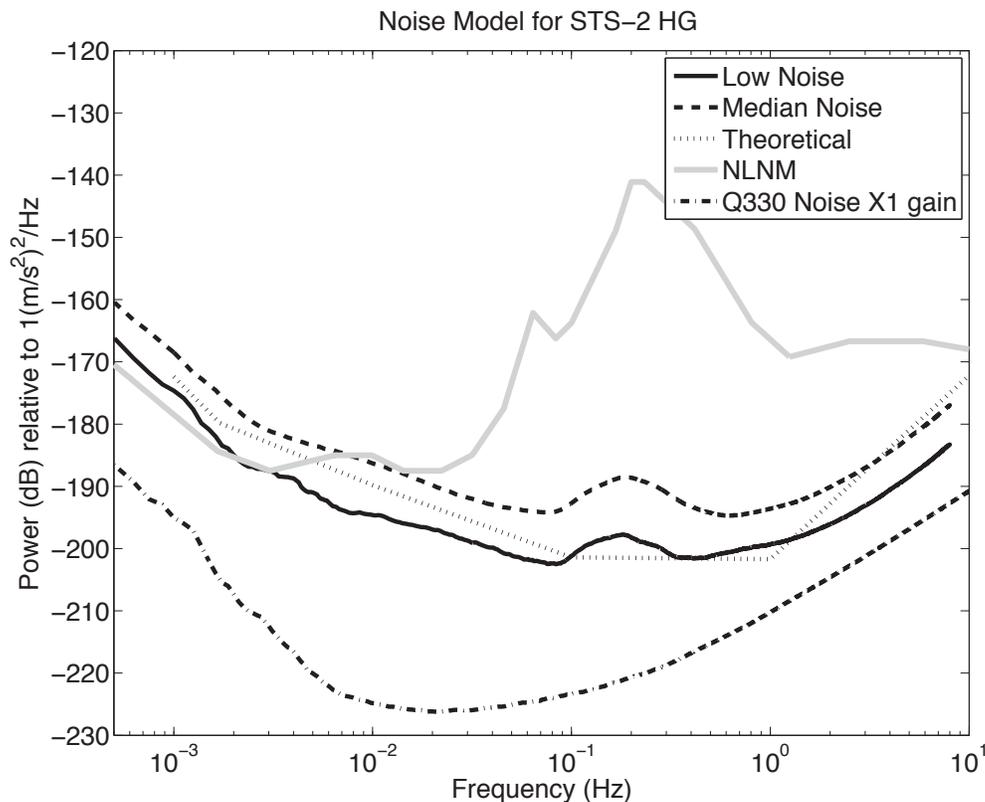
▲ Figure 12. Self-noise model of the Streckeisen STS-2 HG seismometer compared to the theoretical noise model for the STS-2 HG.

coherence analysis method used (Ringler *et al.* forthcoming). In order to get robust measurements it is also important that the sensors be collocated, since the assumption of the self-noise estimate is that all three sensors have a common input signal. Since this assumption is possibly violated with the bore-hole seismometers tested (which were separated by ~30 m), it is possible that their self-noise models are slightly elevated at high frequencies. We did not find any systematic differences in instrument self-noise estimates at low frequencies based on the location of the instrument's low-frequency corner. However, when estimating self-noise it is desirable to use instruments with similar expected noise characteristics (Hutt *et al.* 2009). We also did not find any systematic differences between the vertical component of Galperin tri-axial suspension seismometers and traditional vertical component seismometers. Regardless of suspension type the elevated self-noise estimates in the microseism band do indicate that small misalignment errors contribute to the self-noise in the frequency band with the highest power levels (Holcomb 1990).

We have compared all of our low and median self-noise models (Figures 13 and 14, respectively) with the GSN noise model (Berger *et al.* 2004). At low frequencies, an instrument's self-noise is generally within a few dB of its power spectra (Figure 1). The similar aggregate noise levels between the GSN noise model and the self-noise model of the STS-1 at low frequencies (<0.001 Hz) gives an argument for the robustness of our self-noise models. That is, we would not expect to see large differences in our instrument self-noise models had we

conducted our tests at GSN site locations that may be quieter in the long-period band (*e.g.* GSN station BFO [Black Forest Observatory, Schiltach, Germany] or GSN station PFO [Pinon Flat, California, U.S.A.]).

By calculating self-noise models for both the STS-1 and STS-2 HG seismometers, we see that there is approximately a 7-dB difference in noise levels between the sensors at 1 mHz (Figures 11 and 12). This difference in noise level is smaller than noted by Sleeman *et al.* (2006) and Widmer-Schnidrig (2003). However, it is larger than that noted by Berger *et al.* (2004). Possible causes for these differences in noise levels have been attributed to the quality of installation of the sensors and the variable quality of the STS-2 seismometer (Sleeman *et al.* 2006). In our study we tested the STS-2 HG seismometer in 13 different tests. These 13 different tests included four different installation methods and a total of eight different STS-2 HG seismometers. We believe the diversity of tests and sensors used helps to exclude the above-mentioned possible causes for the differences in the self-noise of the STS-1 and STS-2 HG seismometers at 1 mHz.

ACKNOWLEDGMENTS
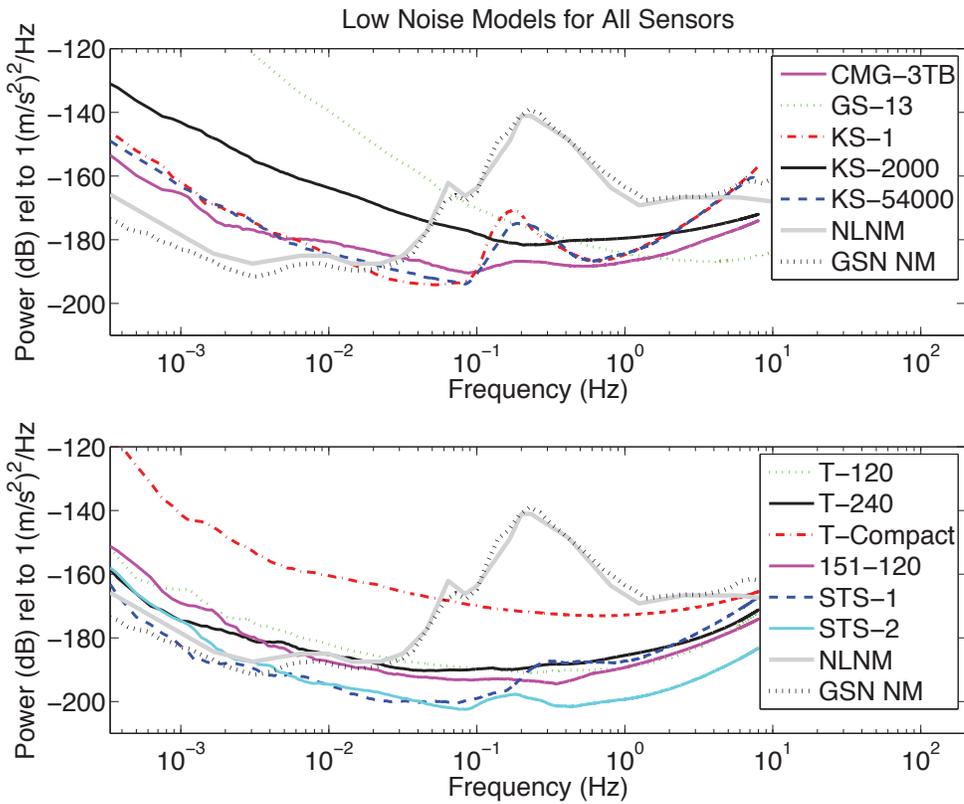
▲ **Figure 13.** Low self-noise models for all seismometers in the study.
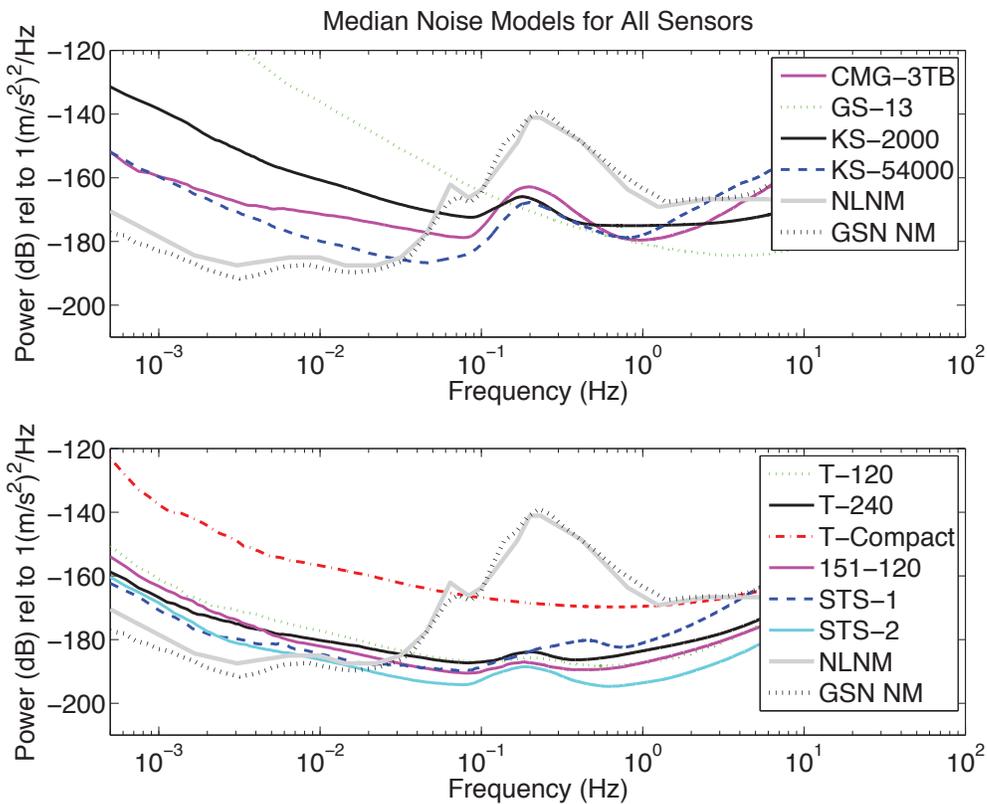
▲ **Figure 14.** Median self-noise models for all sensors in the study. We have not included a median self-noise model for Geotech's KS-1 because of insufficient data.

reviewer, L. Astiz, L. G. Holcomb, and R. A. Uhrhammer for very detailed and helpful reviews of this manuscript that ultimately improved the presentation. ◣

REFERENCES

Berger, J., P. Davis, and G. Ekström (2004). Ambient Earth noise: A survey of the global seismographic network, *Journal of Geophysical Research*, **109**, B11307, doi:10.1029/2004JB003408.

Evans, J. R., F. Followill, C. R. Hutt, R. P. Kromer, J. M. Steim, R. L. Nigbor, A. T. Ringler, and E. Wielandt (2010). Method for calculating self-noise spectra and operating ranges for seismographic inertial sensors and recorders, *Seismological Research Letters*, **81**, (4), 640-646.

Geotech Instruments (1999). *Operation and Maintenance Manual Portable Short-period Seismometer, Model GS-13, Stock Number 990-55400-9800*, 50 pps.

Geotech Systems (2004). *Borehole Seismometer System Model 54000-0103 Operation and Maintenance Manual, Part Number 990-54000-9803*.

Geotech Systems (2006). *Broadband Seismometer Models KS-2000 and KS-2000M operation manual*, 30 pps.

Guralp Systems (2006). *CMG-3TB Operator's Manual, Part MAN-BHO-0001, Issue C*, 78 pps.

Holcomb, L. G. (1989). *A Direct Method for Calculating Instrument Noise Levels in Side-by-Side Seismometer Evaluations*, USGS Open-File Report 89-214, 34 pps.

Holcomb, L. G. (1990). *A Numerical Study of Some Potential Sources of Error in Side-by-Side Seismometer Evaluation*, USGS Open-File Report 90-406, 41 pps.

Hutt, C. R., R. L. Nigbor, and J. R. Evans, eds. (2009). *Proceedings of the Guidelines for Seismometer Testing Workshop, Albuquerque, New Mexico, 9–10 May 2005 ("GST2")*, USGS Open-File Report 2009-1055, 48 pps.

Laske, G. (2004). The needs for/of low-frequency seismology. *IRIS broadband instrumentation workshop*: http://www.iris.edu/stations/seisWorkshop04/abstracts/laske-abstract.pdf.

McNamara, D. E. and R. P. Buland (2004). Ambient noise levels in the continental United States, *Bulletin of the Seismological Society of America*, **94** (4), 1,517-1,527.

Nanometrics (2005). *Trillium 240 seismometer user's guide, Part 15672R3*, 42 pps.

Nanometrics (2006). *Trillium 120P seismometer user's guide, Part 15149R3*, 44 pps.

Nanometrics (2009). *Trillium Compact seismometer user's guide, Part 16889R1*, 67 pps.

Peterson, J. (1993). Observations and Modeling of Seismic Background Noise, USGS Open-File Report 93-322, 94 pps.

Quanterra (1993). *Q680/SXS-G Operation documentation for software release 34/02-RL1231s*, 144pps.

Quanterra (2007). *Q330 Operations guide: Q330HR/Q330 operation overview of support tools baler operation, Document 304808*, 318 pps.

Ref Tek (2010). *151 Broadband Seismometer Operations,* 53 pps.

Rodgers, P. W. (1994). Self-noise for 34 common electromagnetic seismometer/preamplifier pairs, *Bulletin of the Seismological Society of America*, **84** (1), 222-228.

Ringler, A. T., J. R. Evans, C. R. Hutt, L. D. Sandoval (forthcoming). A comparison of instrument self-noise analysis techniques. *Bulletin of the Seismological Society of America.*

Shapiro, N.M., M. Campillo, L. Stehly, and M.H. Ritzwoller (2005). High resolution surface wave tomography from ambient seismic noise, *Science*, **307** (5,715), 1,615-1,618.

Sleeman, R, A. van Wettum, and J. Trampert (2006). Three-channel correlation analysis: A new technique to measure instrumental noise of digitizers and seismic sensors, *Bulletin of the Seismological Society of America*, **96** (1), 258-271.

Streckeisen, G. (1987). *Very-broad-band Feedback Seismometers, STS-1 V/VBB and STS-1 H/VBB Manual*, 46 pps.

Streckeisen, G. (1995). *Portable Very-broad-band Tri-axial Seismometer STS-2 Low-Power Manual*, 50 pps.

Welch, P. D. (1967). The use of fast Fourier transform for the estimation of power spectra: A method based on time averaging over short, modified Periodograms. *IEEE Transactions on Audio and Electroacoustics* AU-15, 70–73.

Widmer-Schnidrig, R. (2003). What can superconducting gravimeters contribute to normal-mode seismology?, *Bulletin of the Seismological Society of America*, **93** (3), 1,370-1,380.

Wielandt, E. (2002*).* Seismic sensors and their calibration. In *New Manual of Seismological Observatory Practices*, 1–46. GeoForschungsZentrum Potsdam. is http://www.gfz-potsdam.de/portal/

Wilson, D., J. Leon, R. Aster, J. Ni, J. Schlue, S. Grand, S. Semken, S. Baldridge, and W. Gao (2002). Broadband seismic background noise at temporary seismic station observed on a regional scale in the southwestern United States, *Bulletin of the Seismological Society of America*, **92** (8), 3,335-3,342.

U.S. Geological Survey
Albuquerque Seismological Laboratory
P.O. Box 82010
Albuquerque, New Mexico 87198-2010 U.S.A.
aringler@usgs.gov
(A. R.)

APPENDIX

In order to remove large variations in our noise estimates and construct sensor self-noise models, we employed a moving average where the number of points averaged is based on the number of points that have not yet been averaged in the power spectra. A similar smoothing method has been used for two-sensor self-noise estimates (Holcomb 1989). The assumption used in the smoothing method is that since there are fewer power spectra values at low frequencies, one does not want to bias the low-frequency end of the power spectra by averaging these points with high-frequency power spectra values.

Suppose the length of our power spectrum, to which we want to apply our smoothing, is of length m, and we want to smooth by 25% of the remaining length. Let $x(n)$ denote the nth value in our power spectra and let $r = 0.25(m − n)$. We further assume that $x(n)$ is ordered so that $x(1)$ is the highest frequency value and our power spectra is ordered in terms of decreasing frequency. Then the averaged value $y(n)$ for $x(n)$, when $n > r$ is given by taking the mean of the values $x(n − r)$, $x(n − r + 1)$, ..., $x(n + r − 1)$, $x(n + r)$. In order to deal with the high-frequency points, where there are not enough points of higher frequency that are still lower than the Nyquist number to be averaged, one can apply a forward difference or simply remove those points.